A Hybrid Dynamical Model for Robotic Underwater Vehicles when Submerged or Surfaced: Approach and Preliminary Evaluation

James E. Hunt and Louis L. Whitcomb

Abstract—This paper reports a numerical method for modeling underwater vehicle (UV) interactions with the free surface using a finite-dimensional dynamical plant model. Although finite-dimensional plant models of fully submerged UV behavior are well-established, they are unable to model the ubiquitous condition of a UV operating at or near the free surface. We report a Monte Carlo-based hybrid model approach for calculating the buoyancy and righting moment of a partially or fully submerged UV in order to model interactions with the free surface. We also report a preliminary evaluation of the hybrid model in numerical simulations, comparing the hybrid model's performance to that of a model for fully submerged UVs and to the experimentally observed behavior of an actual vehicle while fully submerged and while interacting with the free surface. The results of this preliminary study suggest that the proposed hybrid approach may offer a simple and practical method for modeling UV behavior when submerged or interacting with the free surface.

I. Introduction

This paper addresses the problem of finite-dimensional dynamical modeling of underwater vehicles (UVs) while fully submerged or interacting with the free surface. Most previously reported finite-dimensional models for UV dynamics only address the case where the UV is fully submerged and do not address the case where the UV interacts with the free surface. We report a hybrid approach to this problem, and a preliminary evaluation of this approach comparing its performance to that of a standard fully submerged model and to experimentally observed behavior of an actual vehicle.

Advances in UV design, navigation, control, and sensor systems are enabling a variety of novel UV missions that were previously considered impractical or infeasible. Such missions include biological surveys of the water column, which hosts a significant fraction of the Earth's biomass and directly affects the global carbon cycle [24]; national security missions both at sea and in littoral waters, enhancing operations for port security, reconaissance, and rapid event response [14], [18], [22]; and commercial applications, including the survey and inspection of civil infrastructure such as seafloor telecommunication cables and pipelines, and offshore windfarms [23]. A study by the U.S. National Research Council articulated the need for the sustained development of advanced UVs in support of oceanographic research and societal needs throughout the next decade [1].

The development and operation of UV systems benefit from accurate second-order dynamical plant models. During

We gratefully acknowledge the support of the National Science Foundation under Award 1909182.

The authors are with the Department of Mechanical Engineering, Johns Hopkins University, Baltimore, MD, USA 1lw, jhunt40@jhu.edu

the development of UV systems, dynamical models can be employed to simulate UV performance in advance of actual manufacturing and to evaluate the effects of vehicle design variations on vehicle performance. When planning the deployment of UV systems, dynamical models can be used for numerical simulations of the mission to evaluate mission performance in advance of actual mission execution. Dynamical models can also be utilized in model-based control systems and model-based state estimation systems to enable advanced control and navigation of UVs [9].

UV dynamical modeling takes three general approaches: computational fluid dynamics (CFD) modeling, strip theory modeling, and finite-dimensional modeling.

CFD approaches to UV dynamical modeling compute the direct numerical solution to the incompressible Navier-Stokes equation in order to calculate the force and moments on a fully submerged, rigid, 6-degree of freedom (DOF) UV body arising from its interaction with the surrounding infinite-dimensional viscous fluid. CFD is most commonly applied to modeling fully submerged UVs, as CFD for the case of UV interactions with the free surface is non-trivial.

Strip theory approaches are commonly used in numerical simulations of surface ships. Strip theory approaches use a finite-dimensional, 6-DOF plant model and estimate the added mass terms, the radiation and drag force terms, and the buoyancy and righting moment terms of the UV, which are used as forces and moments acting on a conventional second-order finite-dimensional plant model.

Finite-dimensional, second-order dynamical plant models for fully submerged vehicles (without strip theory) are widely utilized with simple closed-form constant-parameter approximations for mass and added mass terms, quadratic drag terms, and buoyancy and righting moment terms. These models are linear in the plant parameters of mass and added mass, quadratic drag, buoyancy, and actuator parameters. The constant model parameters can be estimated with CFD simulations or, as is more commonly done, estimated experimentally in free-motion or captive-motion experiments. While CFD and strip theory approaches require a knowledge of the shape of the vehicle's hull, finite-dimensional dynamical models of fully submerged UVs do not require modeling the UV shape if the plant parameters are estimated experimentally. In general, CFD is a computationally intensive approach for modeling UV dynamics, strip theory is computationally intensive but typically less so than CFD, and finite-dimensional dynamical modeling is usually the least computationally intensive of the three approaches.

Simple finite-dimensional dynamical models of fully sub-

merged UVs are widely utilized for simulating UV motion [9], [11], [16] and for developing model-based control methods [11], [17], [21] and model-based state estimation methods [9], [12], [13]. However, simple finite-dimensional dynamical models of fully submerged UVs do not capture the effects of UV interactions with the free surface and thus cannot model the ubiquitous condition of a vehicle operating at or near the free surface. As a result, these models cannot be used for forward simulations, model-based control, or model-based state estimation for the case of vehicles interacting with the free surface. Given that UVs frequently interact with the free surface when deployed (e.g. to surface in order to obtain a GPS fix at the beginning and end of tracklines during precision surveys), there is a need to develop a finite-dimensional dynamical model capable of modeling interactions with the free surface.

This paper reports a numerical method for modeling the buoyancy force and righting moment of UV interactions with the free surface in a finite-dimensional dynamical model. The method uses Monte Carlo integration to estimate the volume of a UV that is submerged and to estimate the location of the center of buoyancy at any given point during a dive, which in turn yields an estimate of the vehicle's buoyancy force and righting moment. We conjecture that for the common case of UVs that are slightly positively buoyant and whose advance velocity (speed) is low while operating at the free surface, the free surface principally affects the model's buoyancy force and righting moment term, such that the free surface's effect on the added mass and drag terms can be neglected. This approach, if successful, may be less computationally intensive than CFD and strip theory approaches. We report a preliminary evaluation of the proposed approach where we compare its performance to that of a standard dynamical modeling approach for fully submerged vehicles and to the experimentally observed behavior of an actual vehicle.

The remainder of this paper is organized as follows: Section II reviews the history of the development of finitedimensional plant models for fully submerged UVs and a commonly accepted form thereof. Section III reports a novel numerical approach to modeling the plant's interaction with the free surface. Section IV reports a preliminary evaluation of the proposed approach through comparisons to a standard dynamical modeling approach for fully submerged vehicles and to the experimentally observed behavior of an actual vehicle. Section V summarizes and concludes.

II. REVIEW OF 6-DOF UV DYNAMICAL MODELS

This Section briefly reviews the history of 6-DOF UV dynamical modeling and common approaches used today.

A. History of the Development of Finite-Dimensional Plant Models For Underwater Vehicles

The dynamics of a rigid-body UV includes the finitedimensional dynamics of the rigid-body vehicle body itself and the infinite-dimensional dynamics of the fluid surrounding the vehicle. While the former can be described by a finite-dimensional ordinary differential equation (ODE), the latter is described by the infinite-dimensional, incompressible

Navier-Stokes equation. With the exception of a few special cases, the infinite-dimensional Navier-Stokes equation has no closed-form solution and, for the case of marine vehicles, generally cannot be solved numerically in real time [15].

The most commonly accepted finite-dimensional models for submarine vehicles trace their lineage to studies beginning in the late 1950s and early 1960s at the U.S. Navy's David Taylor Model Basin, [7], [10]. In [6] and [2] the authors expanded upon these equations, which have since become widely known as the "Standard equations of motion for submarine simulation" [6] and the "DTNSDC revised standard submarine equations of motion" [2]. Fossen in [3], [4] expanded upon these earlier studies to express the equations of motion in matrix-vector form.

B. Strip Theory for Modeling Surface Vessels

Traditional approaches for modeling surface vessel dynamics rely on strip theory. In strip theory based approaches, the hull of a vessel is modeled as a set of axial sections or "strips", such that the added mass parameters, radiation and drag terms, and buoyancy and righting moment terms are calculated for each strip, and these individual terms can be summed to obtain the aggregate terms for the entire vessel, which are used as forces and moments acting on a conventional second-order finite-dimensional plant model [19].

C. Finite-Dimensional Plant Models

This Section reviews the most commonly accepted finitedimensional plant model for fully submerged UVs. Define the body-frame as a vehicle-fixed, right-handed coordinate system such that its origin is coincident with the vehicle's center of mass (COM), its x-axis points toward the vehicle's bow parallel to the vehicle's longitudinal axis, and its y-axis points to the vehicle's starboard side parallel to the vehicle's lateral axis. Define the world-frame to be a North-East-Down (NED) inertial frame.

The vehicle position and orientation $\mathbf{x} \in \mathbb{R}^6$ is defined as

$$\mathbf{x} = \begin{bmatrix} s^T & \varphi^T \end{bmatrix}^T, \qquad (1)$$

$$s = \begin{bmatrix} x & y & z \end{bmatrix}^T, \quad \varphi = \begin{bmatrix} \phi & \theta & \psi \end{bmatrix}^T, \qquad (2)$$

$$s = \begin{vmatrix} x & y & z \end{vmatrix}^T, \quad \varphi = \begin{vmatrix} \phi & \theta & \psi \end{vmatrix}^T,$$
 (2)

where $s \in \mathbb{R}^3$ denotes the world-frame position in meters and $\varphi \in \mathbb{R}^3$ denotes the attitude (roll, pitch, heading) of the body-frame in Euler angles with respect to the world-frame.

The UV kinematics are

$$\left|\dot{s}^T \quad \dot{\varphi}^T\right|^T = J(\varphi)v,$$
 (3)

where $\dot{s} \in \mathbb{R}^3$ denotes the UV's world-frame linear velocity in meters per second, and $\dot{\varphi} \in \mathbb{R}^3$ denotes the angular velocity of the vehicle-fixed body-frame in Euler rates with respect to the world-frame. Additionally, $v \in \mathbb{R}^6$ denotes the body-frame velocity vector comprised of the bodyframe linear velocity in meters per second and the bodyframe angular velocity in radians per second. $J(\varphi)$ can be expressed explicitly as

$$J(\varphi) = \begin{bmatrix} R(\varphi) & 0\\ 0 & L(\varphi) \end{bmatrix},\tag{4}$$

where $R(\varphi) \in SO(3)$ denotes the transformation from body-frame coordinates to world-frame coordinates and $L(\varphi) \in \mathbb{R}^{3\times 3}$ denotes the transformation from body-frame angular velocities to Euler rates [5]. The vehicle state is composed of the world-frame pose x and the body-frame velocity v.

Finite-dimensional dynamical models of fully submerged UV dynamics are well established [3], [4], [5], [20]. The most commonly accepted second-order equation of motion for fully submerged UVs is

$$M\dot{v} + C(v)v + D(v)v + g(\varphi) = \tau(v, \xi), \tag{5}$$

where $M \in \mathbb{R}^{6 \times 6}$ denotes the inertia matrix, $C(v) \in \mathbb{R}^{6 \times 6}$ denotes the centripetal and Coriolis matrix, $D(v) \in \mathbb{R}^{6 \times 6}$ denotes the hydrodynamic drag matrix, $g(\varphi) \in \mathbb{R}^6$ denotes the buoyancy and righting moment term, and $\tau(v,\xi) \in \mathbb{R}^6$ denotes the control force and moment term which maps the body-frame velocity vector v and the UV's m actuator control commands $\xi \in \mathbb{R}^m$ (which may include propeller angular velocities and/or the angles of articulated control surfaces) to a vector of control forces and moments.

Simple constant-parameter finite-dimensional models for fully submerged UVs require knowledge of the constant plant parameter values (which are most commonly determined experimentally) and are valid for fully submerged vehicle operations. Finite-dimensional plant models are applicable to a wide number of fully submerged use-cases, such as model-based navigation, control, performance simulation, fault detection, and parameter identification. For instance, in [9] the authors report that a dynamical model enabled position estimation for a minimally instrumented autonomous underwater vehicle (AUV), while a simple kinematics-based model failed to yield stable position estimates. Finite-dimensional dynamical models which account for vehicle behavior at the free surface, however, are lacking.

III. A HYBRID 6-DOF UV DYNAMICAL MODEL

This Section reports a numerical approach to model the effects of the free surface on the buoyancy and righting moment term $g(\varphi)$ in (5). For the case of a slightly positively buoyant, substantially submerged UV with a low advance velocity, we conjecture that interactions with the free surface will principally affect the dynamical model's buoyancy and righting moment term, and that interactions with the free surface will have only modest effects on the terms and model parameters associated with added mass, quadratic drag, and control actuators. This approach, if successful, may apply to a wide range of UVs and may model the motion for UVs whose physical dimensions, COM, and model parameters for mass and added mass, drag, and actuators are known.

A. Buoyancy and Righting Moment Model

The buoyancy and righting moment term for fully submerged vehicles, denoted by $g_s(\varphi) \in \mathbb{R}^6$, [3], [4], [5], [20], is commonly expressed as

$$g_s(\varphi) = \begin{bmatrix} (\rho \nabla_s - m) g R(\varphi)^T e_3 \\ \rho g \nabla_s (r_s \times R(\varphi)^T e_3) \end{bmatrix}, \tag{6}$$



Fig. 1. The 100 meter depth-rated Iver3 AUV is one of several commercially available small AUVs designed for oceanographic survey operations including biological, physical-oceanographic, and bathymetric survey missions.

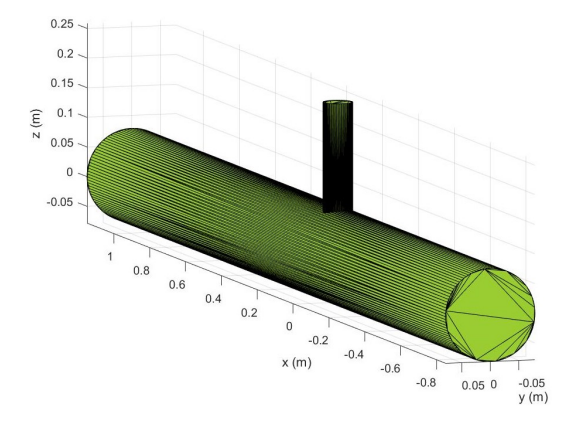


Fig. 2. Bounding volume used to generate a point cloud in the shape of the JHU Iver3 AUV for Monte Carlo integration. The two cylinders were generated as alphaShapes in MATLAB using the approximate dimensions of the vehicle's mast and hull.

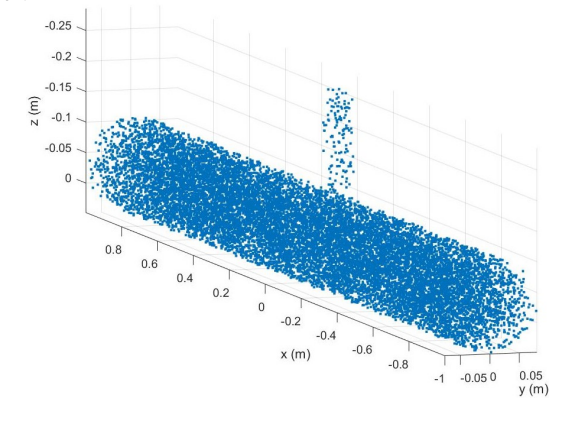


Fig. 3. Point cloud in the shape of the JHU Iver3 AUV composed of points that were randomly generated within the bounding volume for Monte Carlo integration.

where $\rho \in \mathbb{R}$ denotes water density in kilograms per cubic meter, $\nabla_s \in \mathbb{R}$ denotes the UV's constant water volume displacement when fully submerged in cubic meters, $g \in \mathbb{R}$ denotes the acceleration due to gravity in meters per second squared, $m \in \mathbb{R}$ denotes the mass of the UV in kilograms, $R(\varphi) \in SO(3)$ denotes the rotation transformation from body-frame coordinates to world-frame coordinates, $r_s \in \mathbb{R}^3$ denotes the constant position of the fully submerged UV's center of buoyancy relative to the body-frame in meters, and $e_3 = [0,0,1]^T$ denotes the z unit vector.

In order to model UV behavior near the free surface, the buoyancy and righting moment term can be reformulated to account for cases where the UV is partially submerged. Specifically, the constant water displacement volume term for the case of a fully submerged vehicle, denoted by ∇_s

in (6), can be replaced by a time-varying term $\nabla_h(t) \in \mathbb{R}$, which denotes the water displacement volume for the case of a UV whose water volume displacement changes throughout the dive as the vehicle becomes more or less submerged. Similarly, the constant position of the fully submerged UV's center of buoyancy, denoted by r_s in (6), can be replaced by a time-varying term $r_h(t) \in \mathbb{R}^3$, which denotes the position of the center of buoyancy relative to the body-frame for the case of a UV whose center of buoyancy changes throughout the dive as the vehicle becomes more or less submerged. Here, $\nabla_h(t)$ and $r_h(t)$ are defined as functions of time t in order to emphasize that these terms are time-varying, unlike ∇_s and r_s , which are time-invariant. The buoyancy and righting moment term can then be formulated in terms of the time-varying terms $\nabla_h(t)$ and $r_h(t)$ as

$$g_h(\varphi) = \begin{bmatrix} (\rho \nabla_h(t) - m) g R(\varphi)^T e_3 \\ \rho g \nabla_h(t) (r_h(t) \times R(\varphi)^T e_3) \end{bmatrix}. \tag{7}$$

When the vehicle is fully submerged, $\nabla_h(t) = \nabla_s$ and $r_h(t) = r_s$. Under this condition, (7) is mathematically identical to (6), and the two formulations will compute identical buoyancy forces and righting moments.

B. Numerical Approximation of the Center of Buoyancy and Displaced Water Volume

In order to calculate the buoyancy and righting moment term $g_h(\varphi)$, we employ a Monte Carlo integration approach to approximate both $r_h(t)$ and $\nabla_h(t)$. The first step of the approach is to generate a bounding volume with approximately the same dimensions as the UV. For instance, the bounding volume for a torpedo-shaped UV, such as the JHU Iver3 AUV, Fig. 1, may be approximated as a cylinder with approximately the same dimensions as the Iver3's hull and a cylinder with approximately the same dimensions as the Iver3's mast, as shown in Fig. 2. The second step is to generate a set of random points with a uniform isotropic distribution inside the bounding volume, producing a point cloud that approximates the UV's shape, as shown in Fig. 3. These first two steps are performed once at the algorithm's start, and the point cloud may be cached for future use so that it does not need to be regenerated each time the model is evaluated. Then, the water displacement volume $\nabla_h(t)$ can be estimated by calculating the fraction of points from the point cloud which are located below the simulated water surface each time the UV's dynamics are evaluated according to (5) and (7). The vehicle's center of buoyancy $r_h(t)$ can be estimated by calculating the geometric mean of the coordinates of the points from the point cloud which are located below the simulated water surface. The resulting values for $\nabla_h(t)$ and $r_h(t)$ then enable the calculation of $g_h(\varphi)$. Since this approach captures buoyancy and righting moment effects for cases where the UV is partially submerged, it enables calculations of the UV's dynamics when it is interacting with the free surface, as well as when it is fully submerged.

In the sequel, we refer to the UV dynamical plant model (5) and (6), which only models the motion of fully submerged UVs, as the "submerged model." We refer to the UV dynamical plant model (5) and (7), which models the

motion of both fully submerged UVs and the motion of UVs interacting with the free surface, as the "hyrbid model."

IV. HYBRID MODEL PERFORMANCE EVALUATION

This Section reports a preliminary evaluation of the submerged and hybrid models in comparison to actual UV experimental data.

The results reported here were obtained from simulations using the JHU Iver3 AUV models and experiments with the JHU Iver3. The simulations incorporated plant model parameters which were estimated from experimental data, with some manual tuning, to reproduce observed UV behavior. The parameters are listed in Table I. The actuator parameter vector θ_A appearing in Table I is described in [8]. The free surface was modeled as a flat (horizontal) interface parallel to the xy-plane at 0 meters depth. Depth is defined to be positive down. We note that the JHU Iver3's total mass is adjusted (with trim-weights) at the beginning of each dive day for the local water density so that the vehicle is very slightly positively buoyant, with only the antenna mast protruding above the surface and the vehicle nose just touching the surface when the vehicle is at rest on the surface.

TABLE I
DYNAMICAL MODEL PARAMETERS

M	diag([50.5, 70.5, 69.5, 19.8, 109.2, 109.9])
D	$\operatorname{diag}([0.16, 2.44, 12.1, 0.70, 4.04, 0.61]e2) \cdot v $
$(\rho \nabla_s - m)g$	3.53
$r_s \rho \nabla_s g$	[0, 0, -12.5]
θ_A	[1.3, 4.8e-3, 0.68, 1.4, 0.56, 3.1e-5, -5.0e-7]

A. Model Evaluation for Fully Submerged Dives

To verify that the hybrid model performs identically to the submerged model in simulations of dives where the UV is fully submerged, we simulated a dive where the vehicle followed a trackline comprised of four 300 meter legs at depths of 5 meters with turns between tracklines at depths of 4 meters, all with a commanded advance velocity of 1.3 meters per second (2.5 knots). The simulated vehicle was controlled by a standard closed-loop trackline controller for pitch, heading, depth, cross-track, and along-track control. Roll is passively stable and not actively controlled. The individual world-frame position coordinates of the vehicle's COM and attitude coordinates of the body-frame for the submerged and hybrid plant models relative to the worldframe are shown in Fig. 4. The differences between the position and attitude coordinates calculated by the submerged model and those calculated by the hybrid model are also shown in Fig. 4. These differences were calculated as

$$\Delta x = x_{\text{submerged}} - x_{\text{hvbrid}} \tag{8}$$

$$\Delta y = y_{\text{submerged}} - y_{\text{hybrid}} \tag{9}$$

$$\Delta z = z_{\text{submerged}} - z_{\text{hybrid}} \tag{10}$$

$$\Delta \phi = \phi_{\text{submerged}} - \phi_{\text{hybrid}} \tag{11}$$

$$\Delta \theta = \theta_{\text{submerged}} - \theta_{\text{hybrid}} \tag{12}$$

$$\Delta \psi = \psi_{\text{submerged}} - \psi_{\text{hybrid}} \tag{13}$$

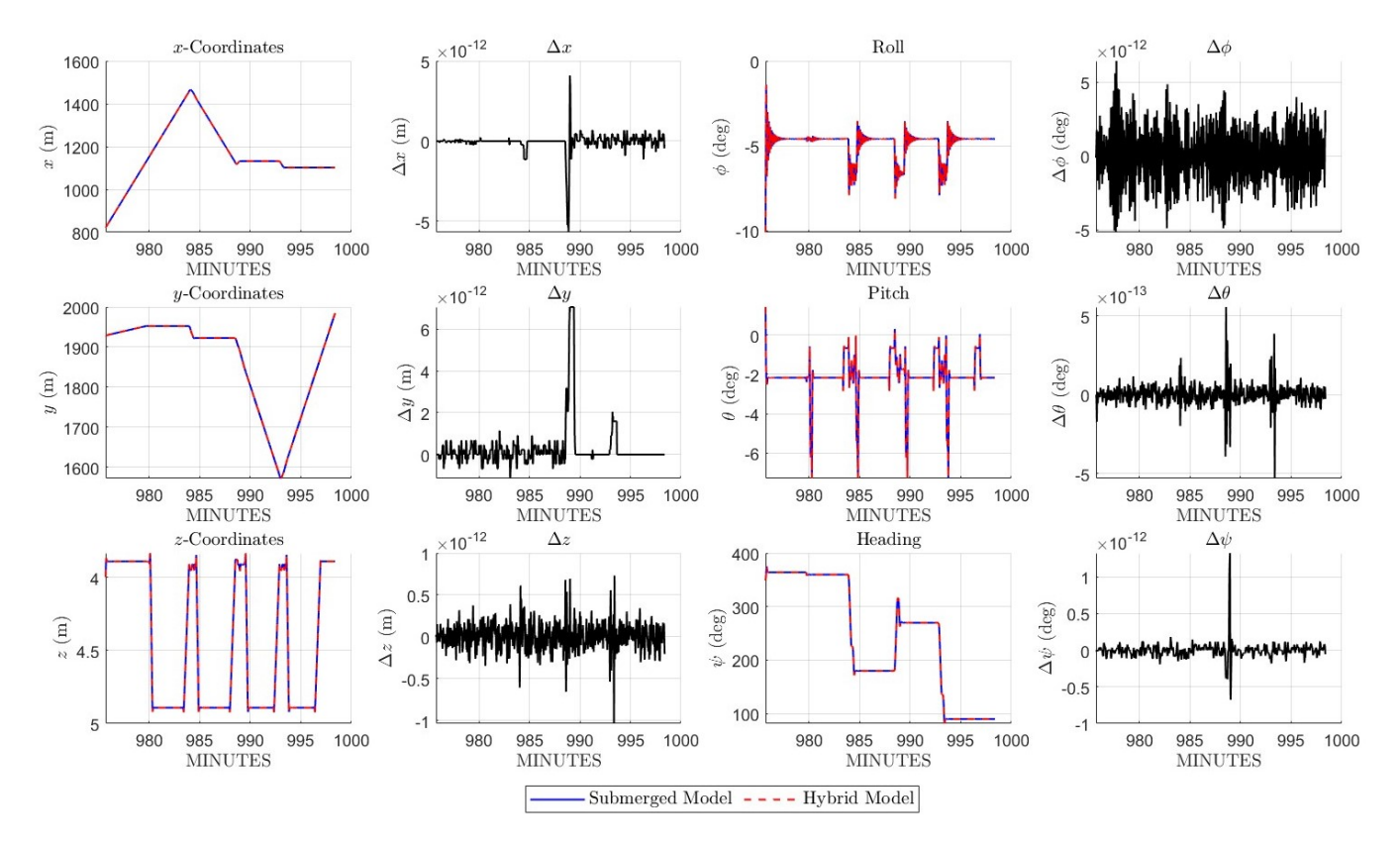


Fig. 4. Fully Submerged Dive: World-frame position coordinates of the UV COM, attitude coordinates of the vehicle-fixed body-frame relative to the world-frame, and the difference in the results calculated by the submerged model and hybrid model for a dive in which the vehicle is fully submerged. The x-axes of each plot describe time in minutes since midnight.

where the model used to calculate each signal is noted with a subscript. Figure 4 shows the results calculated by the submerged and hybrid model differ by no more than 1×10^{-11} meters or degrees for all six degrees of freedom, which is a numerically insignificant difference due to the finite precision of double-precision computation. These results illustrate that for the case of simulating a fully submerged vehicle, the hybrid model performs identically to the submerged model.

B. Model Evaluation for Dives with Surface Interaction

To compare hybrid and submerged model performance with actual vehicle performance, we compared the results of simulated near-surface dives to experimentally measured vehicle data. The experimental data were obtained during a mission with the JHU Iver3 AUV on November 21, 2019 in Round Bay of the Severn River, Maryland. During this mission, the experimental water surface was nearly flat, such that we can reasonably approximate it as a flat surface within our hybrid model approach. The vehicle was programmed to track a waypoint trajectory comprised of four 300 meter legs at depths of 1.2 meters with a desired advance velocity of 1.3 meters per second, separated by turns during which the vehicle would surface to obtain a GPS fix. The simulated dive employed the same waypoints used in the experimental dive. However, since the JHU Iver3 AUV uses a proprietary controller that was unavailable for use in simulation, the simulated controller is not identical to the experimental

controller. In future studies, we intend to further evaluate our approach using a real-world UV that employs the same control algorithm as the simulated UV.

The individual world-frame position coordinates of the vehicle's COM and attitude coordinates of the body-frame relative to the world-frame are shown in Fig. 5. The bottomleft panel of Fig. 5 shows the depth of the vehicle's COM throughout the dive. Figure 5 shows that the depth of the vehicle's COM simulated by the hybrid model does not cross the 0 meter boundary corresponding to the free surface. Rather, the COM of the vehicle simulated by the hybrid model has a steady-state depth of approximately 0.13 meters when it surfaces, which is consistent with the JHU Iver3 AUV depths that were observed when surfaced. In contrast, the vehicle simulated by the submerged model has a steady-state COM depth of approximately -0.2 meters when it surfaces, which corresponds to a depth above the free surface. These results show that the UV depth behavior predicted by the hybrid model accounts for the free surface in a manner that is consistent with experimentally measured vehicle behavior, while the submerged model yields depth behavior that is physically unrealistic.

The middle-right plot of Fig. 5 shows that the pitch of the body-frame predicted by the controlled hybrid model is positive when the vehicle transits along the surface, which is consistent with the experimentally measured pitch. This behavior can be accounted for by the fact that the desired

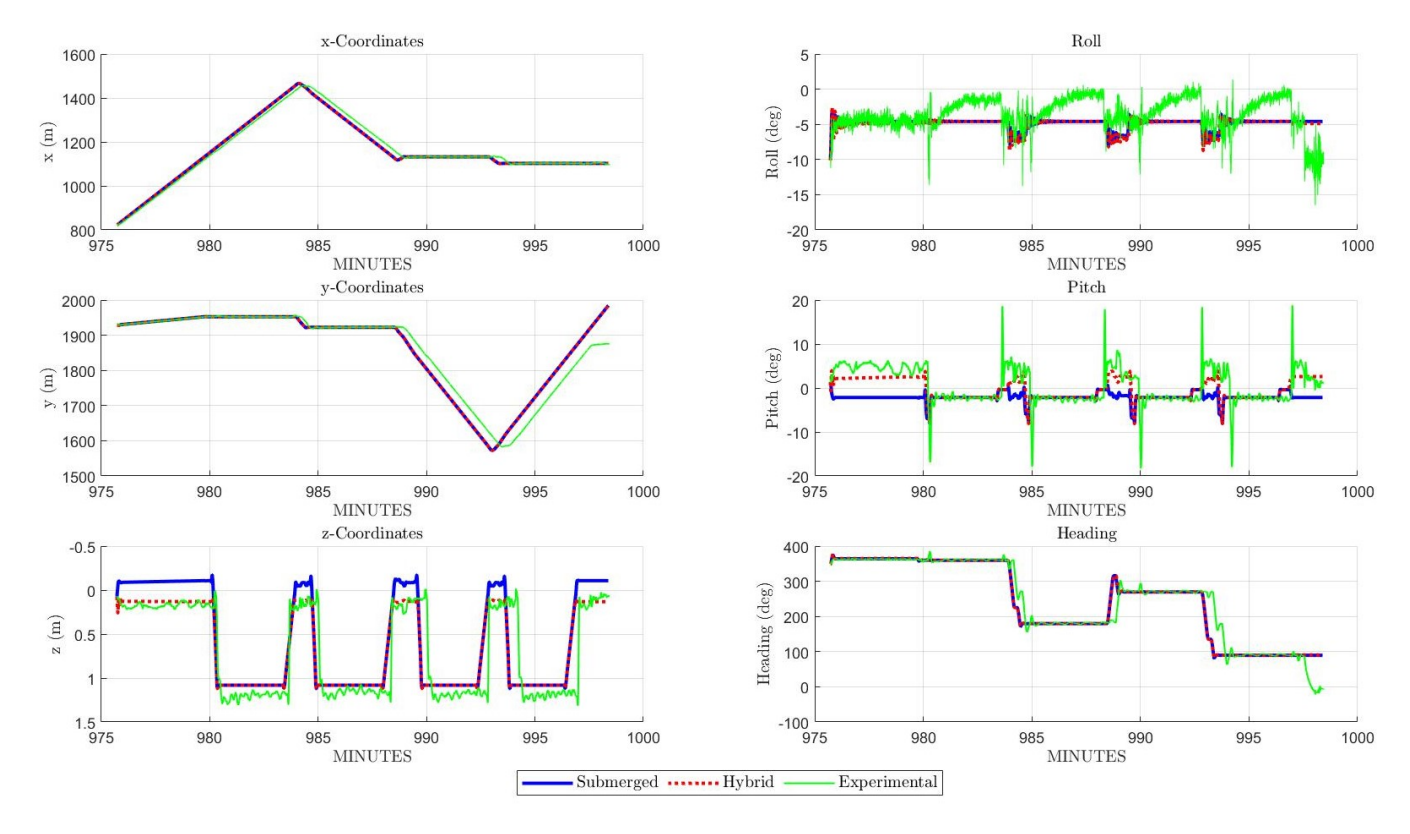


Fig. 5. Dive with Free Surface Interaction: World-frame position coordinates of the UV COM and attitude coordinates of the vehicle-fixed body-frame relative to the world-frame for a dive in which the vehicle surfaces during turns. The x-axes of each plot describe time in minutes since midnight.

depth of the trackline is 0 meters during turns where the vehicle surfaces. As a result, the vehicle will attempt to reach this trackline depth by pitching upwards when transiting along the surface. In contrast, the pitch of the body-frame as predicted by the submerged model is negative during turns when the vehicle is programmed to surface. This behavior can be accounted for by the fact that the JHU Iver3 AUV is slightly positively buoyant, such that it must assume a slightly nose-down attitude (i.e. negative pitch) in order to maintain level flight when fully submerged. Since the submerged model does not account for interactions with the free surface, it will behave as if the vehicle were fully submerged even when it is above the simulated free surface, such that we would expect the controlled submerged model to predict a negative pitch near the free surface.

The submerged model and hybrid model predict similar behavior to one another for the x- and y-coordinates, roll, and heading, which is to be expected since these degrees of freedom are not as significantly influenced by the buoyancy effects of free surface interactions. The top-right plot of Fig. 5 shows that the simulated roll behavior of both models differs by several degrees from the experimentally measured roll behavior. This discrepancy in the roll behavior may be a result of inaccuracies in the model parameters and the fact that roll is not actively controlled in the simulations nor in the JHU Iver3 AUV. The proposed approach still provides a reasonably accurate prediction of the vehicle's roll.

V. CONCLUSIONS

This study reports a numerical approach to modeling UV dynamics which addresses the case of a UV that operates both fully submerged and in interaction with the free surface during its missions. This study also reports a preliminary evaluation of the proposed approach where we compare the performance of both the submerged model and the hybrid model to the experimentally observed behavior of the actual vehicle. Modeling UV interactions with the free surface is of interest as there is a lacuna of simple finite-dimensional dynamical models which can model the ubiquitous condition of a UV operating at or near the free surface. The preliminary performance evaluation reported herein suggests that our proposed approach may offer a simple method for modeling UV behavior at and near the free surface.

ACKNOWLEDGEMENTS

We gratefully acknowledge the contribution of Zachary J. Harris and Tyler M. Paine who provided the MATLAB implementation of the fully-submerged vehicle dynamics model and the adaptively identified model parameters, which serve as the basis for the development of the hybrid surface-interaction vehicle dynamics model reported herein. We also gratefully acknowledge the support of Mr. Rick and Ms. Valerie Smith, owners of Smiths Marina, Crownsville, MD, for their gracious support of the JHU Iver3 AUV experimental sea trials reported herein.

REFERENCES

- [1] N. R. Council, Critical In frastructureforOcean Needs 2030. Washing-Research and Societal in DC: The National Academies Press, 2011. [Onton. https://nap.nationalacademies.org/catalog/13081/ line]. Available: critical-infrastructure-for-ocean-research-and-societal-needs-in-2030
- [2] J. Feldman, "DTNSRDC Revised Standard Submarine Equations of Motion," US Department of Defense, Tech. Rep., 1979. [Online]. Available: https://apps.dtic.mil/sti/pdfs/ADA071804.pdf
- [3] T. I. Fossen, Guidance and Control of Ocean Vehicles. New York, NY: John Wiley and Sons, 1994.
- [4] —, Marine Control Systems: Guidance, Navigation, and Control of Ships, Rigs, and Underwater Vehicles. Trondheim, Norway: Marine Cybernetics, 2002.
- [5] —, Handbook of Marine Craft Hydrodynamics and Motion Control, 2nd Edition. New York, NY: John Wiley and Sons, 2021.
- [6] M. Gertler and G. R. Hagen, "Standard Equations of Motion for Submarine Simulation," David W Taylor Naval Ship Research and Development Center, Bethesda MD, Tech. Rep., 1967. [Online]. Available: https://apps.dtic.mil/sti/citations/AD0653861
- [7] A. Goodman, "Experimental techniques and methods of analysis used in submerged body reseach," in *Proc. of the Third Symposium on Naval Hydromechanics*, Scheveningen, Holland, 1960.
- [8] Z. J. Harris, A. M. Mao, T. M. Paine, and L. L. Whitcomb, "Stable nullspace adaptive parameter identification of 6 degree-of-freedom plant and actuator models for underactuated vehicles:theory and experimental evaluation," *International Journal of Robotics Research*, 2023. Accepted for Publication, In Press.
- [9] Z. J. Harris and L. L. Whitcomb, "Cooperative acoustic navigation of underwater vehicles without a DVL utilizing a dynamic process model: Theory and field evaluation," *Journal of Field Robotics*, vol. 38, no. 5, pp. 700–726, 2021. [Online]. Available: https://onlinelibrary.wiley.com/doi/abs/10.1002/rob.22008
- [10] F. H. Imlay, "The Complete Expressions for Added Mass of a Rigid Body Moving In an Ideal Fluid," David Taylor Model Basin Washington DC, Tech. Rep., 1961. [Online]. Available: https://apps.dtic.mil/sti/citations/AD0263966
- [11] M. V. Jakuba, D. R. Yoerger, and L. L. Whitcomb, "Longitudinal control design and performance evaluation for the *Nereus* 11,000 m underwater vehicle," in *OCEANS* 2007, 2007, pp. 1–10.
- [12] J. C. Kinsey and L. L. Whitcomb, "Model-based nonlinear observers for underwater vehicle navigation: Theory and preliminary experiments," in *Proceedings 2007 IEEE International Conference on Robotics and Automation*, 2007, pp. 4251–4256.
- [13] J. C. Kinsey, Q. Yang, and J. C. Howland, "Nonlinear dynamic model-based state estimators for underwater navigation of remotely operated vehicles," *IEEE Transactions on Control Systems Technology*, vol. 22, no. 5, pp. 1845–1854, 2014.
- [14] A. Kukulya, J. Bellingham, J. Kaeli, C. Reddy, M. Godin, and R. Conmy, "Development of a propeller driven long range autonomous

- underwater vehicle (LRAUV) for under-ice mapping of oil spills and environmental hazards: An arctic domain center of awareness project (ADAC)," in 2016 IEEE/OES Autonomous Underwater Vehicles (AUV), 2016, pp. 95–100.
- [15] L. Larsson, B. Regnstrom, L. Broberg, D. Li, and C. Janson, "Failures, fantasies, and feats in the theoretical/numerical prediction of ship performance," in *Proceedings of the 22nd Symposium on Naval Hydrodynamics*, Washington, DC, USA, 1998, pp. 11–32.
- [16] A. M. Mao and L. L. Whitcomb, "A novel quotient space approach to model-based fault detection and isolation: Theory and preliminary simulation evaluation," in 2021 IEEE/RSJ International Conference on Intelligent Robots and Systems (IROS), 2021, pp. 7119–7126.
- [17] S. C. Martin and L. L. Whitcomb, "Nonlinear model-based tracking control of underwater vehicles with three degree-of-freedom fully coupled dynamical plant models: Theory and experimental evaluation," *IEEE Transactions on Control Systems Technology*, vol. 26, no. 2, pp. 404–414, 2018.
- [18] B. P. McNelly, L. L. Whitcomb, J. P. Brusseau, and S. S. Carr, "Evaluating integration of autonomous underwater vehicles into port protection," in OCEANS 2022, Hampton Roads, 2022, pp. 1–8.
- [19] J. N. Newman, Marine Hydrodynamics. Cambridge, MA: MIT Press, 1977. [Online]. Available: https://mitpress.mit.edu/9780262534826/ marine-hydrodynamics
- [20] T. M. Paine, "Robust Model Identification Methods for Nonlinear Second-Order Plant Models for Underwater Vehicles," Master's thesis, Johns Hopkins University, 2018. [Online]. Available: http://ihir.library.ihu.edu/handle/1774.2/59285
- [21] L. L. Whitcomb, J. C. Howland, D. A. Smallwood, D. R. Yoerger, and T. E. Thiel, "A new control system for the next generation of US and UK deep submergence oceanographic ROVs," *IFAC Proceedings Volumes*, vol. 36, no. 4, pp. 133–138, 2003, IFAC Workshop on Guidance and Control of Underwater Vehicles 2003, Newport, South Wales, UK, 9-11 April 2003. [Online]. Available: https://www.sciencedirect.com/science/article/pii/S1474667017366703
- [22] D. P. Williams, "On optimal AUV track-spacing for underwater mine detection," in 2010 IEEE International Conference on Robotics and Automation, 2010, pp. 4755–4762.
- [23] M. Wright, W. Gorma, Y. Luo, M. Post, Q. Xiao, and A. Durrant, "Multi-actuated auv body for windfarm inspection: Lessons from the bio-inspired robofish field trials," in 2020 IEEE/OES Autonomous Underwater Vehicles Symposium (AUV), 2020, pp. 1–6.
- [24] D. R. Yoerger, A. F. Govindarajan, J. C. Howland, J. K. Llopiz, P. H. Wiebe, M. Curran, J. Fujii, D. Gomez-Ibanez, K. Katija, B. H. Robison, B. W. Hobson, M. Risi, and S. M. Rock, "A hybrid underwater robot for multidisciplinary investigation of the ocean twilight zone," *Science Robotics*, vol. 6, no. 55, p. eabe1901, 2021. [Online]. Available: https://www.science.org/doi/abs/10.1126/scirobotics.abe1901